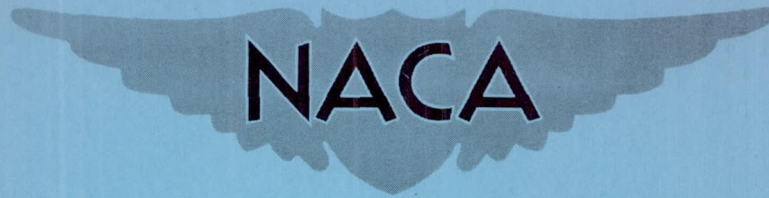


CONFIDENTIAL

Copy 304

RM A53L17

NACA RM A53L17



RESEARCH MEMORANDUM

THE TRANSONIC CHARACTERISTICS OF UNSWEPT WINGS HAVING ASPECT RATIOS OF 4, SPANWISE VARIATIONS IN THICKNESS RATIO, AND VARIATIONS IN PLAN-FORM TAPER -
TRANSONIC-BUMP TECHNIQUE

By Warren H. Nelson

Ames Aeronautical Laboratory
Moffett Field, Calif.

CLASSIFICATION CHANGED TO UNCLASSIFIED

AUTHORITY NACA RESEARCH ABSTRACT NO. 94

DATE: JAN. 11, 1956

CLASSIFIED DOCUMENT

WHL

This material contains information affecting the National Defense of the United States within the meaning of the espionage laws, Title 18, U.S.C., Secs. 793 and 794, the transmission or revelation of which in any manner to an unauthorized person is prohibited by law.

NATIONAL ADVISORY COMMITTEE
FOR AERONAUTICS

WASHINGTON

March 12, 1954

CONFIDENTIAL

NATIONAL ADVISORY COMMITTEE FOR AERONAUTICS

RESEARCH MEMORANDUMTHE TRANSONIC CHARACTERISTICS OF UNSWEPT WINGS HAVING ASPECT
RATIOS OF 4, SPANWISE VARIATIONS IN THICKNESS RATIO,
AND VARIATIONS IN PLAN-FORM TAPER -

TRANSONIC-BUMP TECHNIQUE

By Warren H. Nelson

SUMMARY

An investigation was conducted to determine the effects of spanwise variations in thickness ratio on the aerodynamic characteristics of wings at transonic speeds. The lift, drag, and pitching-moment data are presented for three wings having aspect ratios of 4, taper ratios of 1.0, 0.5, and 0.2, NACA 63A006 sections at the roots, and NACA 63A002 sections at the tips. The Mach number range of the tests was from 0.6 to 1.1, corresponding to a Reynolds number range of 1.4 million to 1.9 million.

The results indicate that near a Mach number of 1.0, the drag of the wings with spanwise variations in thickness ratio and that of wings having constant thickness ratios can be correlated effectively in terms of thickness ratio if a weighted thickness ratio is used.

INTRODUCTION

Systematic research to determine the aerodynamic characteristics of various unswept wings through the transonic speed range has been initiated in the Ames 16-foot high-speed wind tunnel. Investigations to date have been made of symmetrical rectangular wings to determine the effects of aspect ratio and thickness; the results of those tests are reported in references 1 and 2. The effect of camber on rectangular wings having the same aspect ratios and thicknesses was investigated and has been reported in references 3 and 4. The effects of taper in plan form have also been investigated and the results are presented in reference 5.

The purpose of this report is to present that part of the general program involving the effect of spanwise variations of thickness ratio.

Three wings having an aspect ratio of 4 and taper ratios of 1.0, 0.5, and 0.2 were investigated. The wings had thickness ratios of 6 percent at the roots and 2 percent at the tips. The equal-percent-chord stations of the root and tip sections were connected by straight lines.

NOTATION

A	aspect ratio, $\frac{b^2}{S}$
C_D	drag coefficient, $\frac{\text{twice semispan drag}}{qS}$
$C_{D_{\min}}$	minimum drag coefficient
C_{D_f}	friction-drag coefficient, assumed equal to the minimum drag coefficient at 0.6 Mach number
$\left(C_{D_P}\right)_{\min}$	minimum pressure-drag coefficient, assumed equal to $C_{D_{\min}} - C_{D_f}$
C_L	lift coefficient, $\frac{\text{twice semispan lift}}{qS}$
C_m	pitching-moment coefficient, referred to $0.25\bar{c}$, $\frac{\text{twice semispan pitching moment}}{qS\bar{c}}$
$\frac{L}{D}$	lift-drag ratio
$\left(\frac{L}{D}\right)_{\max}$	maximum lift-drag ratio
M	mean Mach number in region of wing
M_L	local Mach number
S	total wing area, twice wing area of semispan model, sq ft
V	velocity, ft/sec
b	twice span of semispan model, ft
c	local wing chord, ft

\bar{c}	mean aerodynamic chord, $\frac{\int_0^{b/2} c^2 dy}{\int_0^{b/2} c dy}$, ft
q	dynamic pressure in region of wing, $\frac{1}{2}\rho V^2$, lb/sq ft
$\frac{t}{c}$	thickness-to-chord ratio
$\overline{\left(\frac{t}{c}\right)}$	weighted thickness-to-chord ratio, $\left[\frac{\int_0^{b/2} \left(\frac{t}{c}\right)^{5/3} c dy}{\int_0^{b/2} c dy} \right]^{3/5}$
y	spanwise distance from plane of symmetry, ft
α	angle of attack, deg
λ	taper ratio, $\frac{\text{tip chord}}{\text{root chord}}$
ρ	air density in region of wing, slugs/cu ft
$\frac{dC_L}{d\alpha}$	slope of lift curve measured at zero lift, per deg
$\frac{dC_m}{dC_L}$	slope of pitching-moment curve measured at zero lift

APPARATUS AND MODELS

The tests were conducted in the Ames 16-foot high-speed wind tunnel utilizing a transonic bump. A description of the transonic bump may be found in reference 6. The forces and moments were measured by means of a strain-gage balance mounted within the bump.

Figure 1 is a photograph of one of the wings mounted on the bump and figure 2 is a sketch of the models. Three wings having aspect ratios of 4, taper ratios of 1.0, 0.5, and 0.2, and equal areas were constructed of steel. The root profile used for each wing was the NACA 63A006, and the tip profile was the NACA 63A002. The constant-percent-chord lines connecting the root and tip sections were straight-line elements. As a result, there was a linear variation of absolute thickness from root to tip. The spanwise variation of thickness ratio in percent chord is shown in figure 3. The tips of the wings were constructed by rotating the tip sections.

A fence 3/16 inch from the bump surface was used to prevent the flow through the gap between the wing support and bump surface from affecting the flow over the wing.

The precision of the data in this report has been established from consideration of repeatability of data for identical conditions. On this basis, the Mach numbers are accurate to ± 0.01 , the lift coefficients are accurate to ± 0.005 , and the drag and pitching-moment coefficients are accurate to ± 0.001 .

TESTS AND PROCEDURE

The lift, drag, and pitching-moment data were obtained for the wings over a Mach number range from 0.6 to 1.1. This Mach number range corresponded to an extreme Reynolds number range of 1.4 million to 1.9 million, based on the mean aerodynamic chord of the wings. In general, the angle-of-attack range was from -2° to the stall, or to where the root bending stress became critical.

A Mach number gradient existed in the flow over the bump where the wings were mounted. Typical contours of the local Mach number over the bump in the absence of the wings are shown in figure 4. Outlines of the wings have been superimposed on the contours to indicate the Mach number gradients which existed over the wings during the tests. No attempt has been made to evaluate the effects of these gradients. The test Mach numbers presented are the mean values in the region of the wings.

The data have been reduced to standard NACA coefficients. A tare correction to the drag was made to account for the drag of the fence and support. The drag tare was evaluated by cutting the wing off flush with the fence and measuring the forces on the fence and support. The interference effects of the fence on the wings and the effects of leakage around the fence are unknown.

RESULTS AND DISCUSSION

The basic lift, drag, and pitching-moment data are presented in figures 5 through 7.

A weighted thickness ratio was used in comparing the wings having spanwise variations in thickness ratio with those having a constant thickness ratio. Since thickness effects have a large influence on the drag in the transonic region, the weighted thickness ratios were determined on the basis of drag. It has been shown in reference 2

that at a Mach number of 1.0, for wings having values of $A(t/c)^{1/3}$ greater than 1.0, the minimum pressure drag varies approximately as the $5/3$ power of the thickness ratio. Equating the drag of a wing having a constant thickness ratio to that for a wing having a spanwise variation in thickness ratio (assuming that the pressure drag varies as the $5/3$ power of the thickness ratio) results in the following weighted thickness parameter:

$$\overline{\left(\frac{t}{c}\right)} = \left[\frac{\int_0^{b/2} \left(\frac{t}{c}\right)^{5/3} c \, dy}{\int_0^{b/2} c \, dy} \right]^{3/5}$$

In the remainder of this report, any discussion of thickness will be on the basis of the weighted thickness parameter. The weighted thickness ratios for the wings having taper ratios of 1.0, 0.5, and 0.2 are 4.1, 4.7, and 5.4 percent, respectively.

The drag coefficient as a function of Mach number for the wings is shown at three lift coefficients in figure 8. The drag coefficient for the wing having a taper ratio of 0.2 was slightly higher than that for the other wings at zero lift and 0.6 Mach number. This difference in drag is probably the result of surface conditions and, to some extent, errors in the drag tares.

In order to correlate the wings better, the minimum pressure-drag coefficient has been plotted as a function of Mach number in figure 9(a). Included in the figure are data from reference 5 for wings having aspect ratios of 4, plan-form taper ratios of 0.5, and constant thickness ratios of 2, 4, and 6 percent. The minimum pressure-drag coefficient at any Mach number was assumed to be equal to the minimum drag coefficient minus the minimum drag coefficient at 0.6 Mach number. The data show an increase in the minimum pressure drag as the thickness was increased. To correlate this drag increase with thickness, the minimum pressure-drag coefficients at Mach numbers of 1.00 and 1.08 are presented as functions of the similarity thickness parameter $\overline{\left(\frac{t}{c}\right)}^{5/3}$ in figure 9(b).

The minimum pressure drags for the wings correlated well with the weighted thickness ratio to the $5/3$ power as shown in figure 9(b). The greatest deviation from the faired line occurs at a Mach number of 1.08 for the wing having a taper ratio of 0.5, and a $\overline{\left(\frac{t}{c}\right)}^{5/3}$ of 0.0061; this deviation amounts to a 6-percent difference in minimum-pressure-drag coefficient. It would appear that the minimum pressure drags for

the wings having spanwise variations in thickness ratio can be correlated effectively with the minimum pressure drags for wings having a constant thickness ratio if a suitable weighted thickness ratio is used. The effect of changes in plan-form taper on the minimum pressure drag (at least for the taper ratios used in this investigation) was small and secondary to thickness effects.

The lift-curve slope as a function of Mach number is shown in figure 10. Included in the figure are lift-curve slopes from reference 5 for wings having aspect ratios of 4, taper ratios of 0.5, and constant thickness ratios of 4 and 6 percent. In comparing the wings having taper ratios of 0.5, on the basis of thickness, it appears that the wings were in sequence at the peak lift-curve slope. The differences in lift-curve slope for the wings having varying spanwise thickness ratios, in general, are small throughout the Mach number range. If the separate effects of thickness and taper are considered using the data of reference 5, the wing having a taper ratio of 0.5 would be expected to have a maximum lift-curve slope approximately 10 percent greater than the wing having a taper ratio of 0.2; however, only about 5-percent increase was realized in this investigation.

The lift-drag ratio is shown as a function of lift coefficient in figure 11. The variation of maximum lift-drag ratio, and lift coefficient for maximum lift-drag ratio, with Mach number is presented in figure 12. The values for maximum lift-drag ratio shown are corrected for the differences in minimum drag at 0.6 Mach number. The minimum drag coefficient for the wing having a taper ratio of 0.2 was corrected so as to be equal to that for the wing with a taper ratio of 1.0. The correction increased the maximum lift-drag ratio from 13.1 to 14.3 at 0.6 Mach number, and from 6.4 to 6.8 at 1.08 Mach number. The wing having a taper ratio of 1.0 and the smallest weighted thickness ratio had the highest lift-drag ratio throughout the Mach number range.

The pitching-moment-curve slope as a function of Mach number is presented in figure 13. The slopes were taken through zero lift. Data from reference 5 for wings having aspect ratios of 4, taper ratios of 0.5 and constant thickness ratios of 2, 4, and 6 percent have been included in the figure for comparison. When the wings having taper ratios of 0.5 are compared, it is seen that the wing having a weighted thickness ratio of 0.047 does not fall into sequence with the wings having constant thickness ratios; however, the differences are small, amounting to a difference in the aerodynamic center equal to about 2 percent of the mean aerodynamic chord. The over-all center-of-pressure travel in going from subsonic to supersonic speeds remained about the same. A comparison of the wings having spanwise variations in thickness ratio indicates that the wing with 0.5 taper ratio had the greatest over-all center-of-pressure travel in going from subsonic to supersonic speeds; however, again the maximum difference was only about 2 percent

of the mean aerodynamic chord. These small differences in center-of-pressure travel in terms of mean aerodynamic chord actually become more significant when the differences in the lengths of the mean aerodynamic chords are considered. Expressing the maximum over-all travel as absolute distance traveled, the wings having taper ratios of 0.5 and 0.2 had 16 and 21 percent greater travel, respectively, than the wing having a taper ratio of 1.0.

CONCLUDING REMARKS

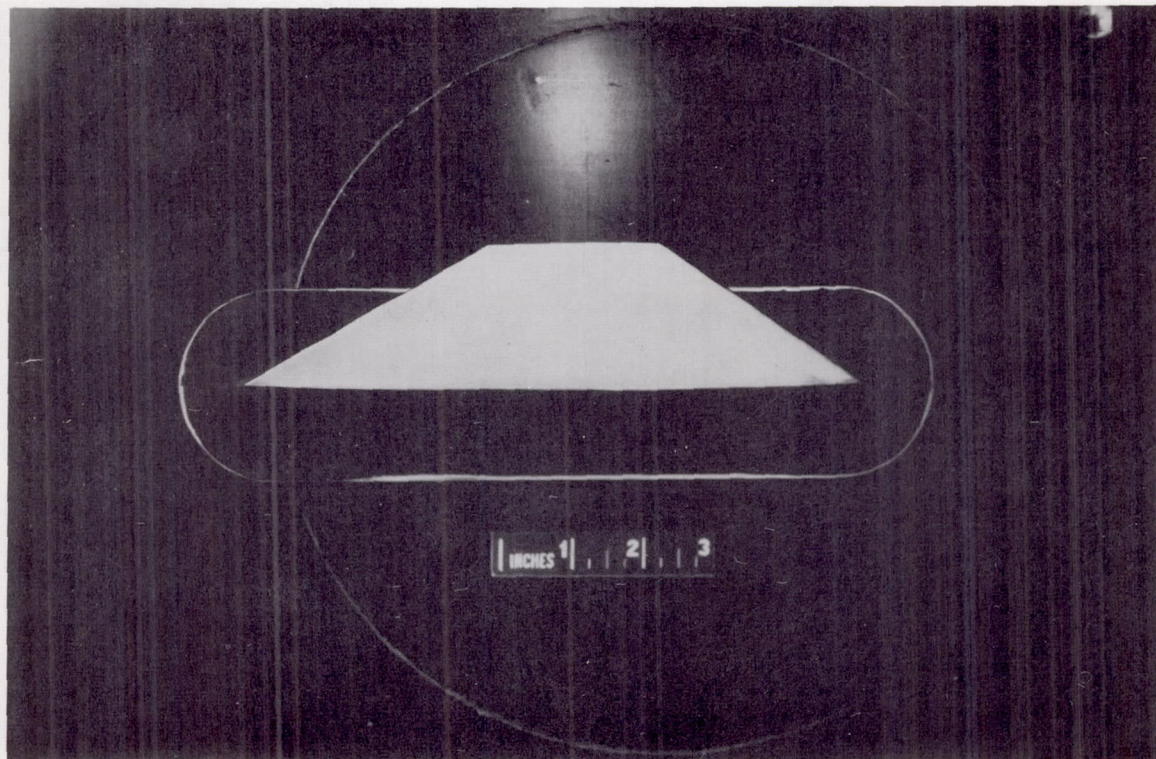
The results of tests to determine the transonic aerodynamic characteristics of three wings having taper ratios of 1.0, 0.5, and 0.2, and spanwise variations in thickness ratios indicate that near a Mach number of 1.0, the drag can be correlated effectively in terms of thickness ratio with the drag of wings having constant thickness ratio when a weighted thickness ratio is used.

Ames Aeronautical Laboratory
National Advisory Committee for Aeronautics
Moffett Field, Calif., Dec. 17, 1953

REFERENCES

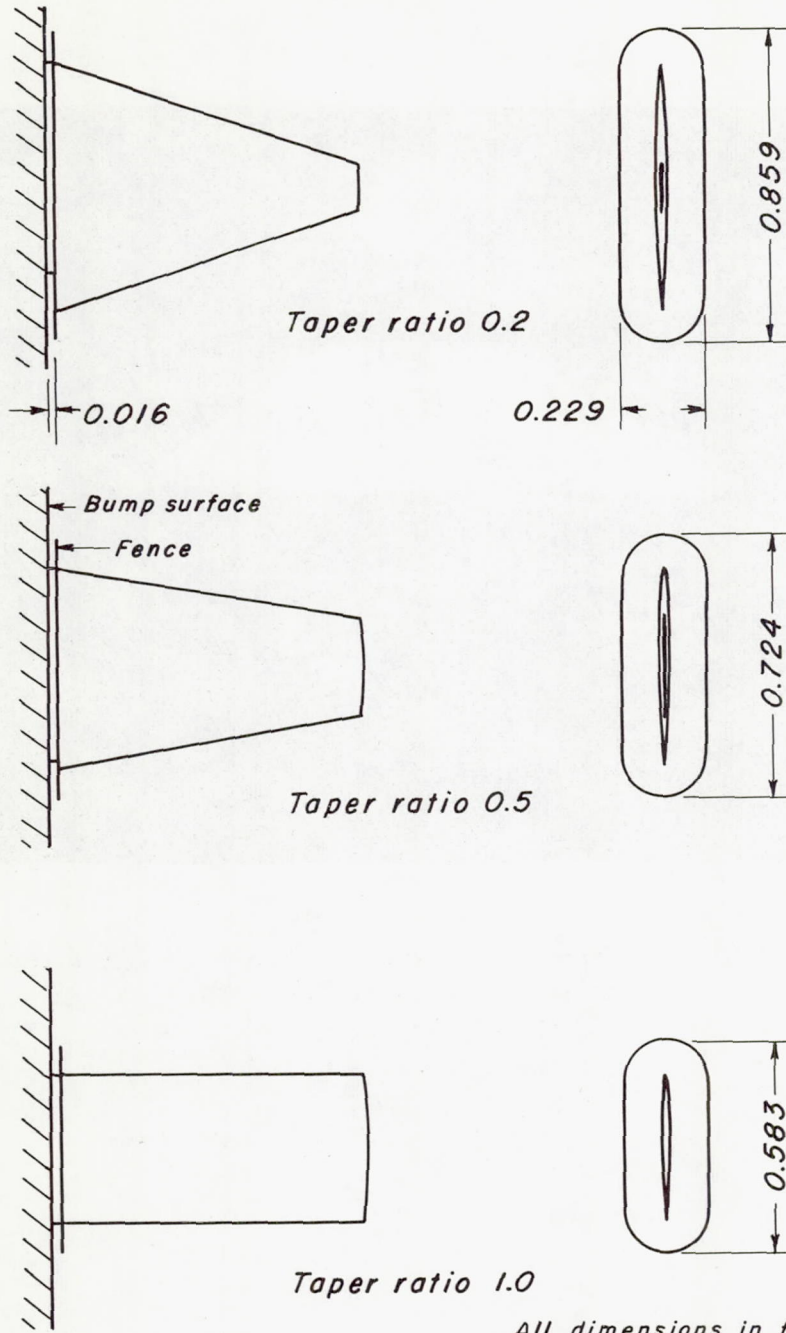
1. Nelson, Warren H., and McDevitt, John B.: The Transonic Characteristics of 17 Rectangular, Symmetrical Wing Models of Varying Aspect Ratio and Thickness. NACA RM A51A12, 1951.
2. McDevitt, John B.: A Correlation by Means of the Transonic Similarity Rules of the Experimentally Determined Characteristics of 22 Rectangular Wings of Symmetrical Profile. NACA RM A51L17b, 1952.
3. Nelson, Warren H., and Krumm, Walter J.: The Transonic Characteristics of 38 Cambered Rectangular Wings of Varying Aspect Ratio and Thickness as Determined by the Transonic Bump Technique. NACA RM A52D11, 1952.
4. McDevitt, John B.: A Correlation by Means of Transonic Similarity Rules of the Experimentally Determined Characteristics of 18 Cambered Wings of Rectangular Plan Form. NACA RM A53G31, 1953.

5. Nelson, Warren H., Allen, Edwin C., and Krumm, Walter J.: The Transonic Characteristics of 36 Symmetrical Wings of Varying Taper, Aspect Ratio, and Thickness as Determined by the Transonic-Bump Technique. NACA RM A53I29, 1953.
6. Axelson, John A., and Taylor, Robert A.: Preliminary Investigation of the Transonic Characteristics of an NACA Submerged Inlet. NACA RM A50C13, 1950.



A-17628.1

Figure 1.- The wing having an aspect ratio of 4 and a taper ratio of 0.2 mounted on the bump.



All dimensions in feet

Taper ratio	Root chord	Tip chord	\bar{c}	Semi-span	Root section	Tip section
0.2	0.694	0.139	0.478	0.833	63A006	63A002
0.5	.555	.278	.432	.833	63A006	63A002
1.0	.417	.417	.417	.833	63A006	63A002

NACA

Figure 2.- Sketches of the wings.

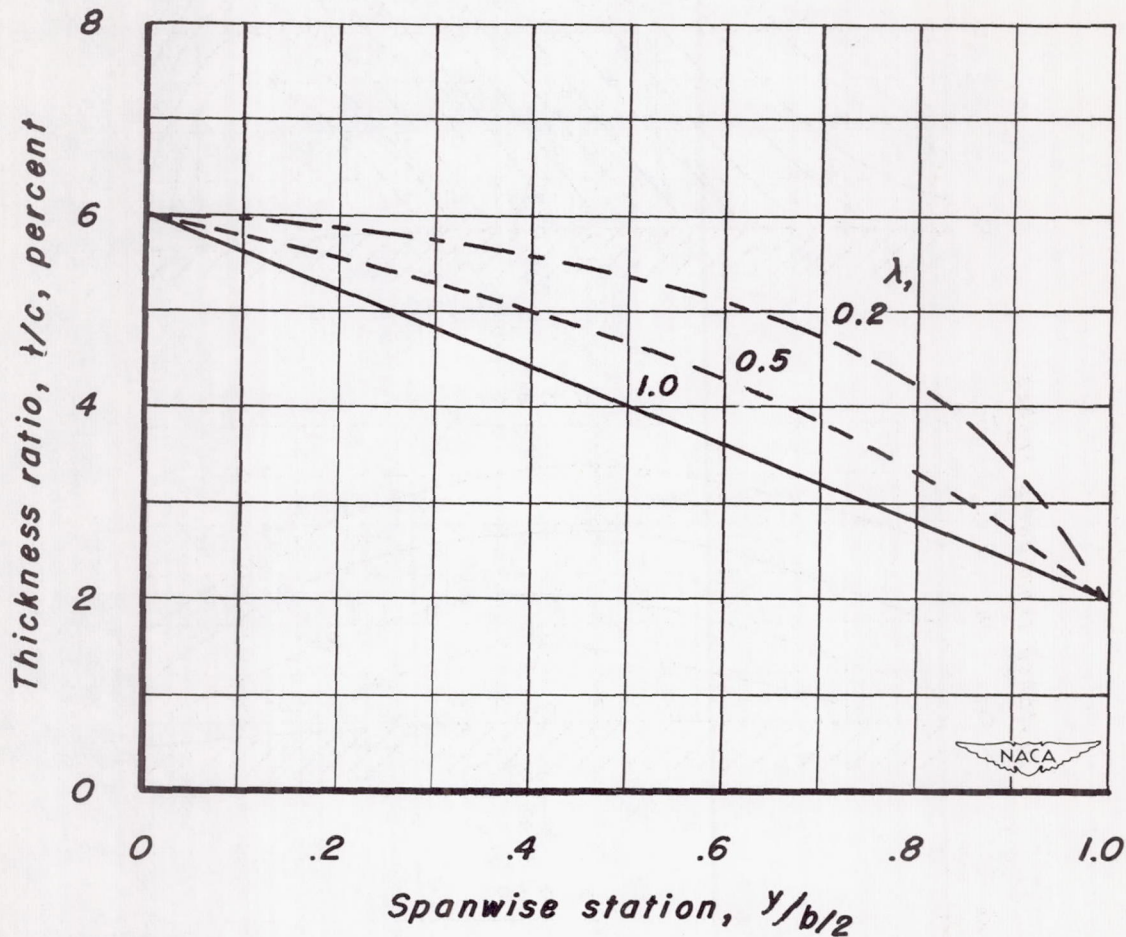


Figure 3.- Spanwise variation of thickness ratio for the wings.

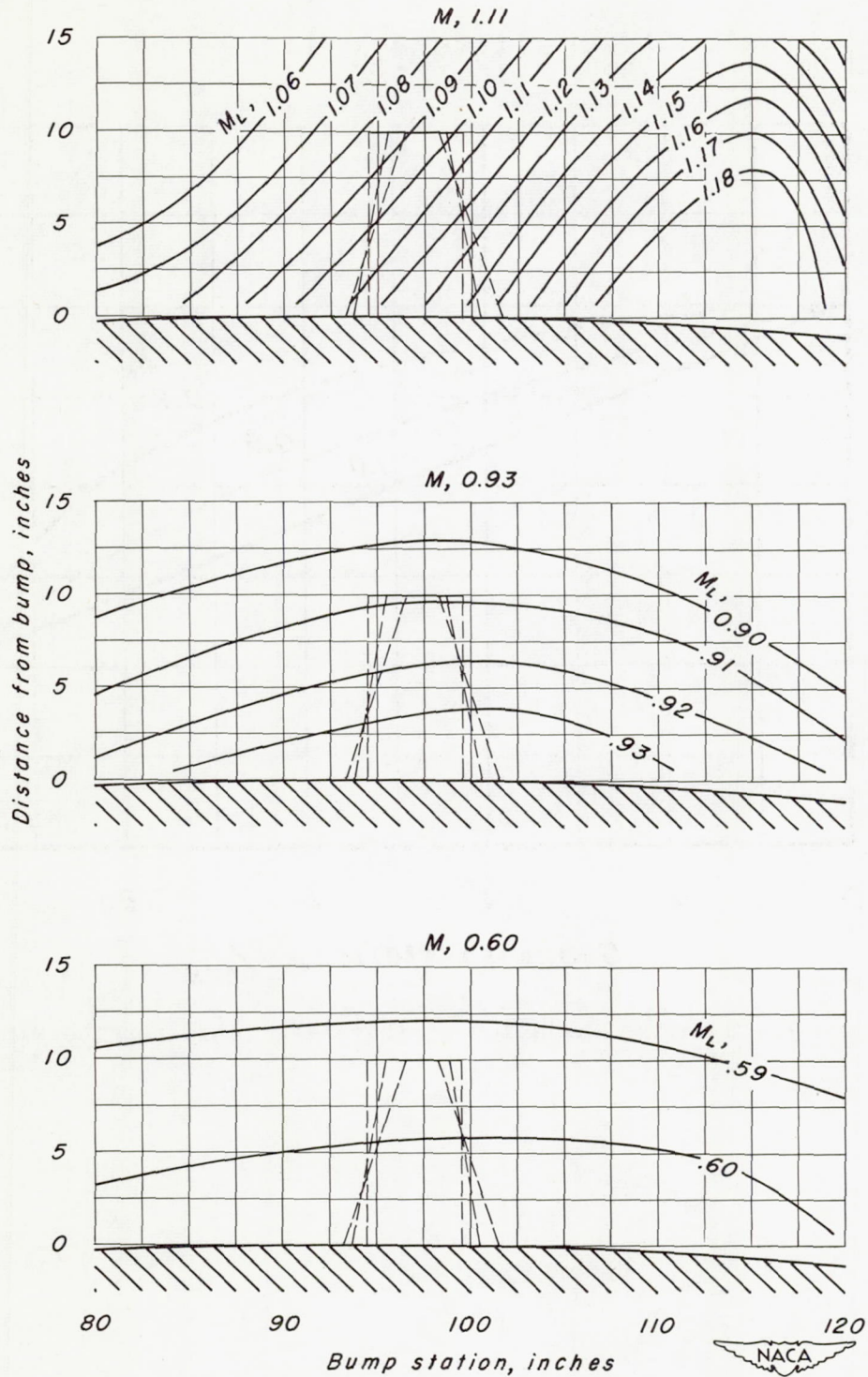
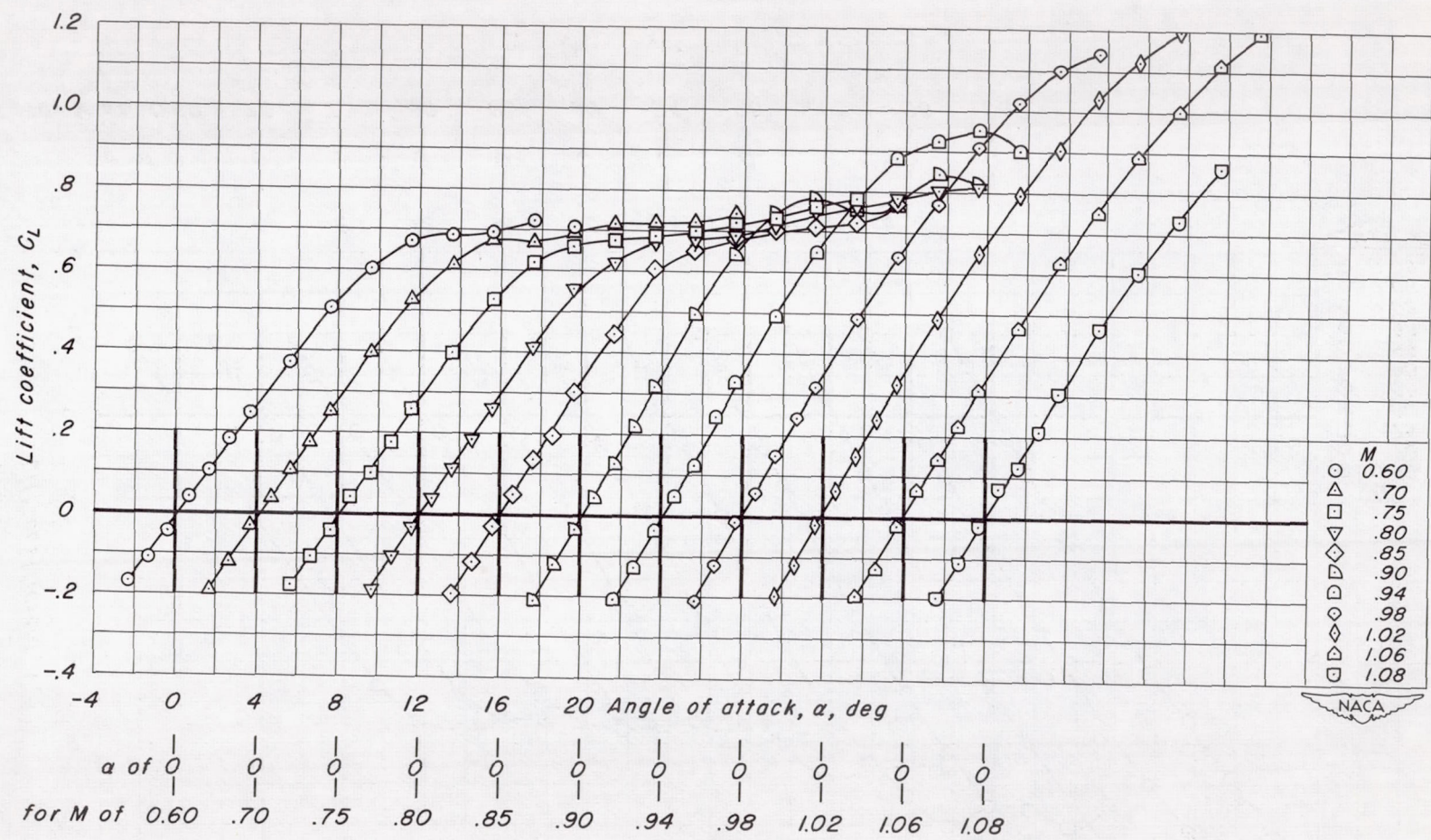


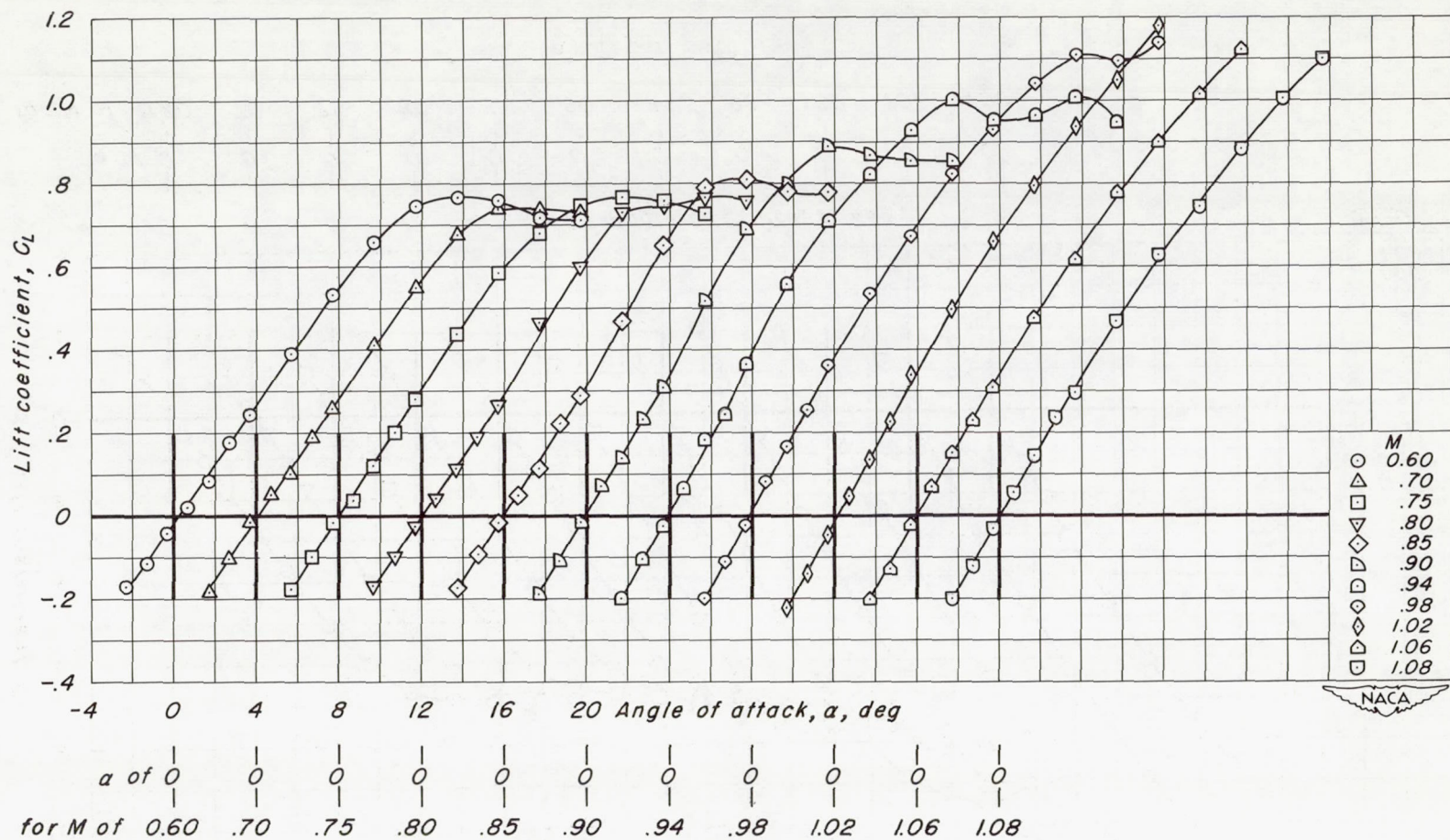
Figure 4.- Typical Mach number contours over the transonic bump in the Ames 16-foot high-speed wind tunnel.

CONFIDENTIAL



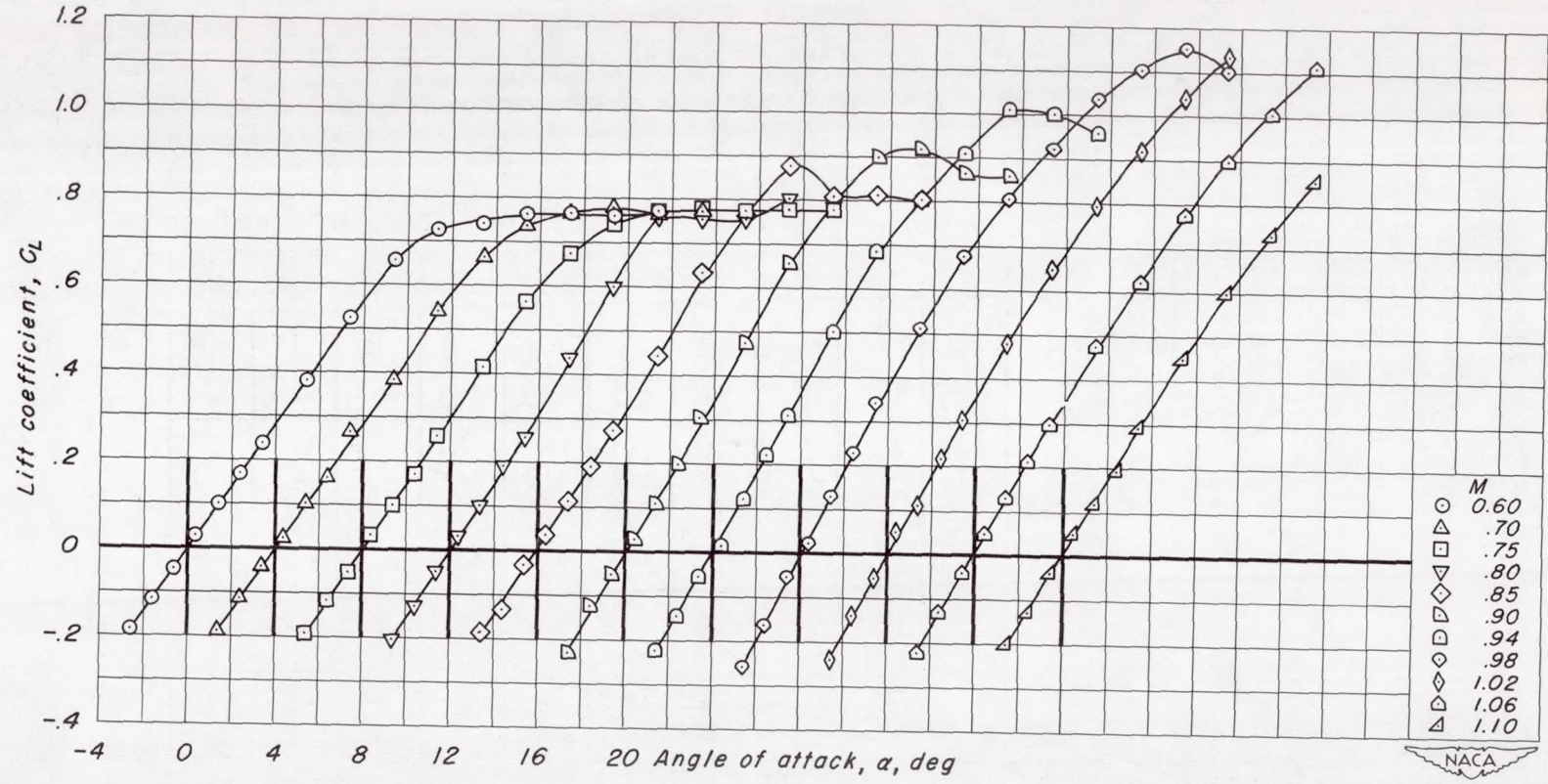
(a) Taper ratio = 0.2

Figure 5.- The variation of lift coefficient with angle of attack.



(b) Taper ratio = 0.5

Figure 5.- Continued.

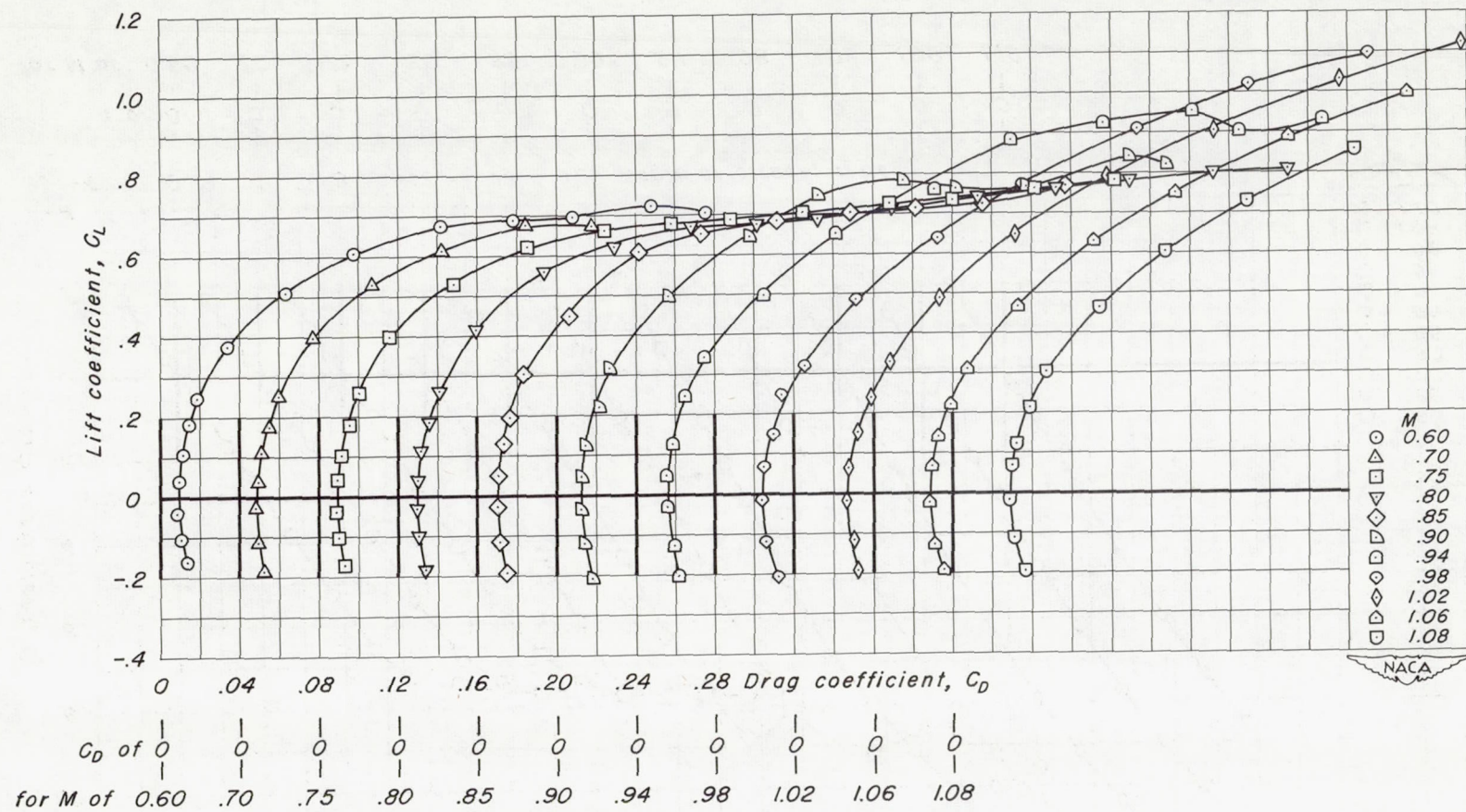


α of 0 | 0 | 0 | 0 | 0 | 0 | 0 | 0 | 0 | 0 | 0
for M of 0.60 | .70 | .75 | .80 | .85 | .90 | .94 | .98 | 1.02 | 1.06 | 1.10

(c) Taper ratio = 1.0

Figure 5.- Concluded.

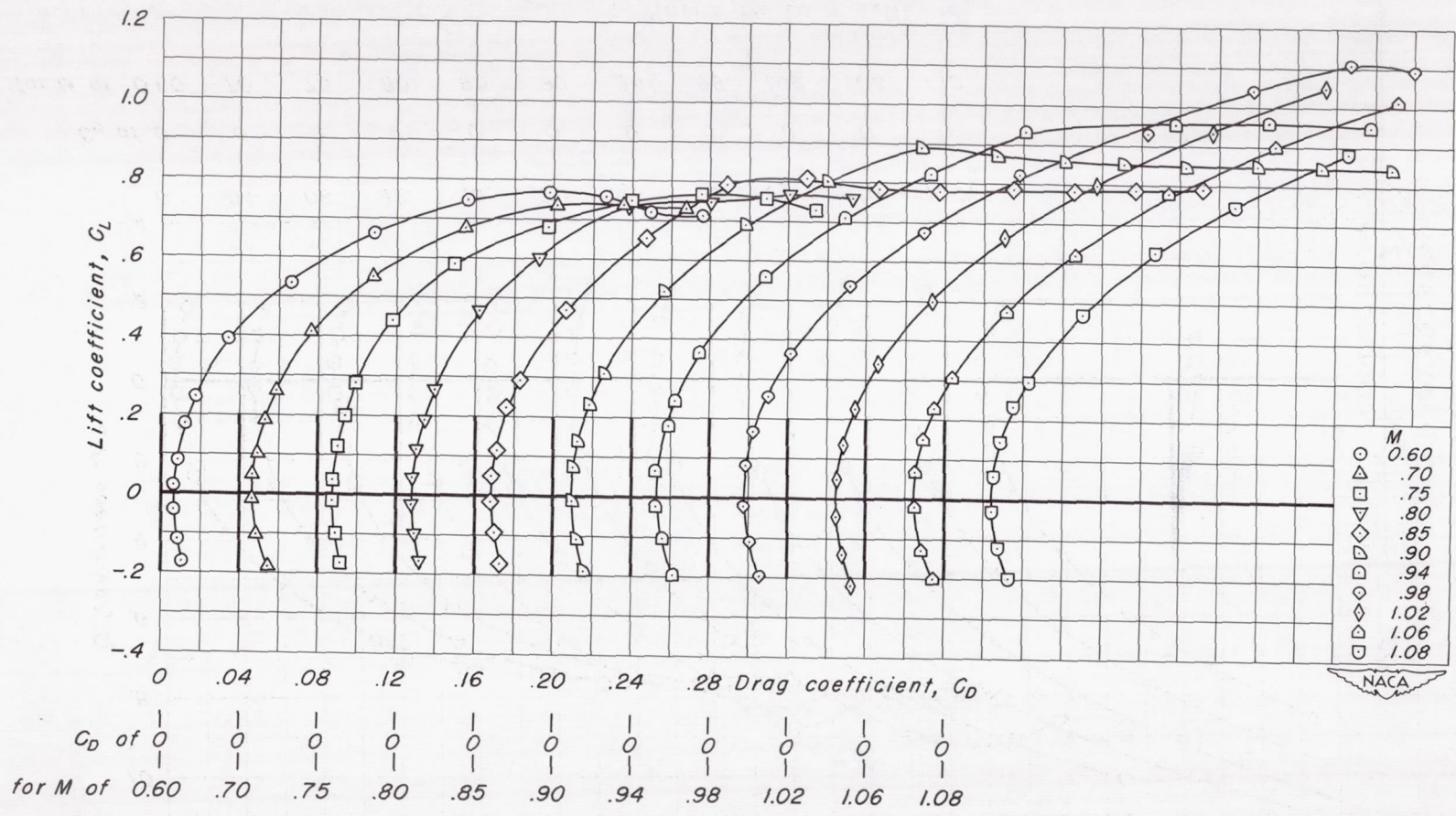
CONFIDENTIAL



(a) Taper ratio = 0.2

Figure 6.- The variation of drag coefficient with lift coefficient.

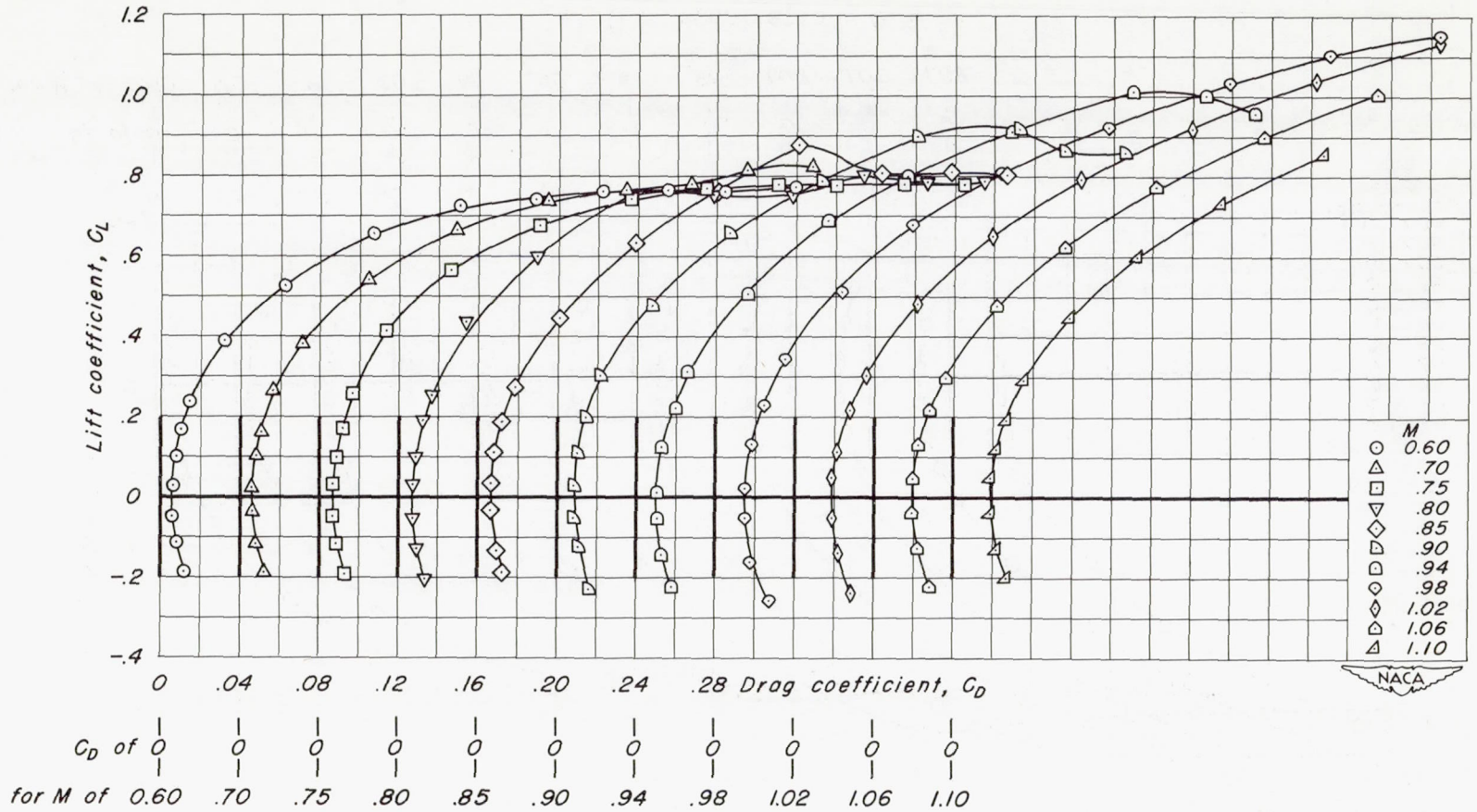
CONFIDENTIAL



(b) Taper ratio = 0.5

Figure 6.- Continued.

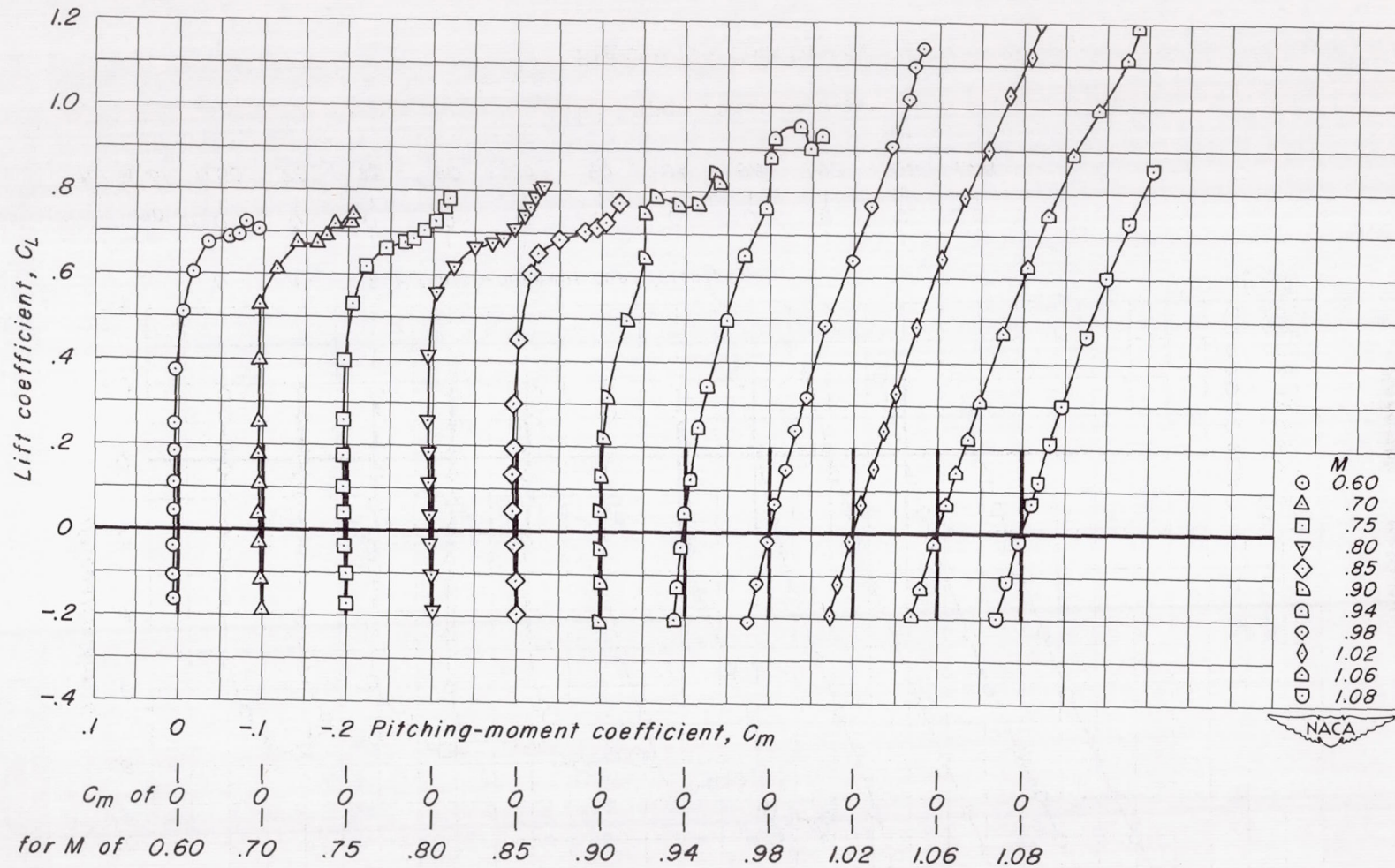
CONFIDENTIAL



(c) Taper ratio = 1.0

Figure 6.- Concluded.

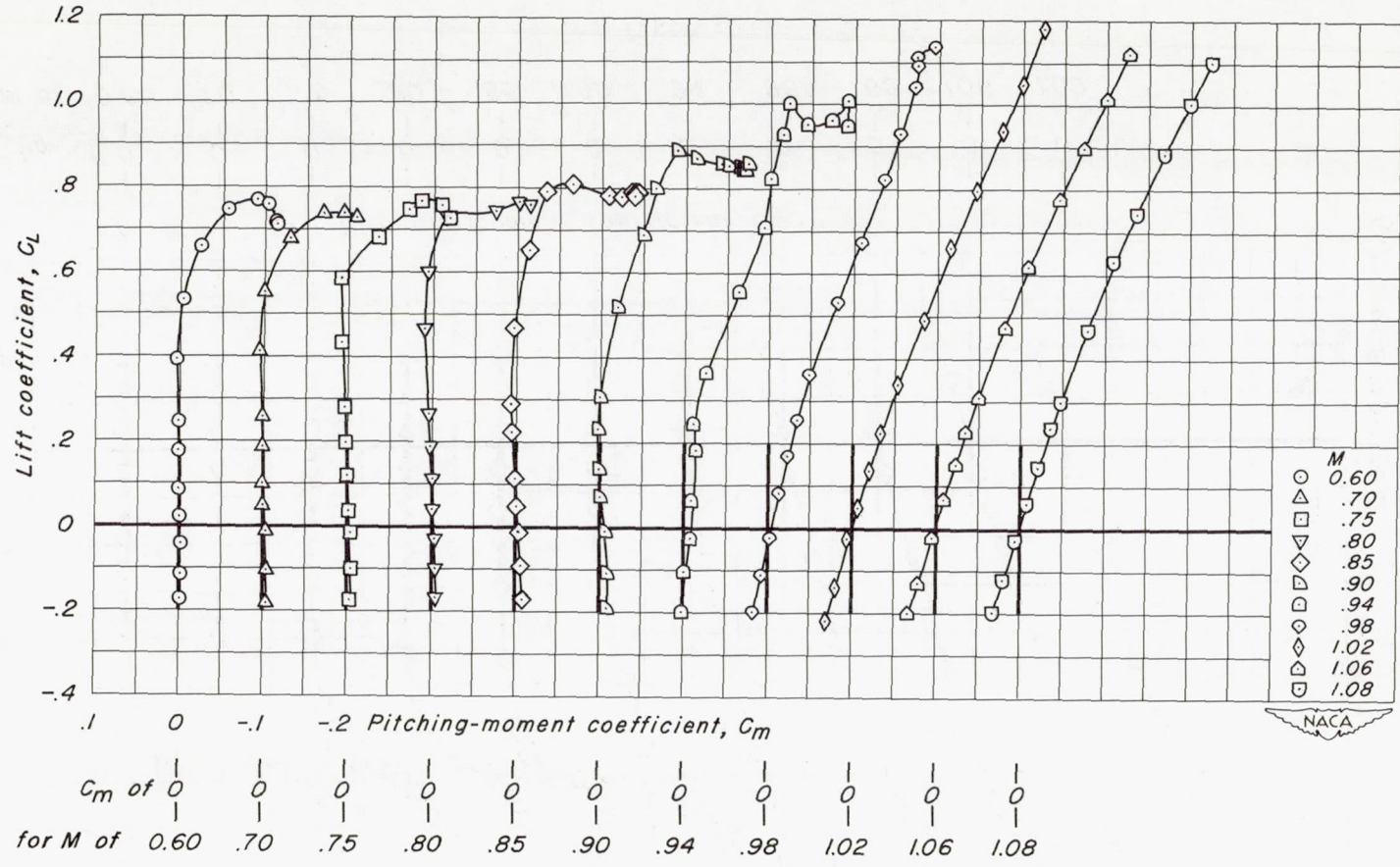




(a) Taper ratio = 0.2

Figure 7.- The variation of pitching-moment coefficient with lift coefficient.

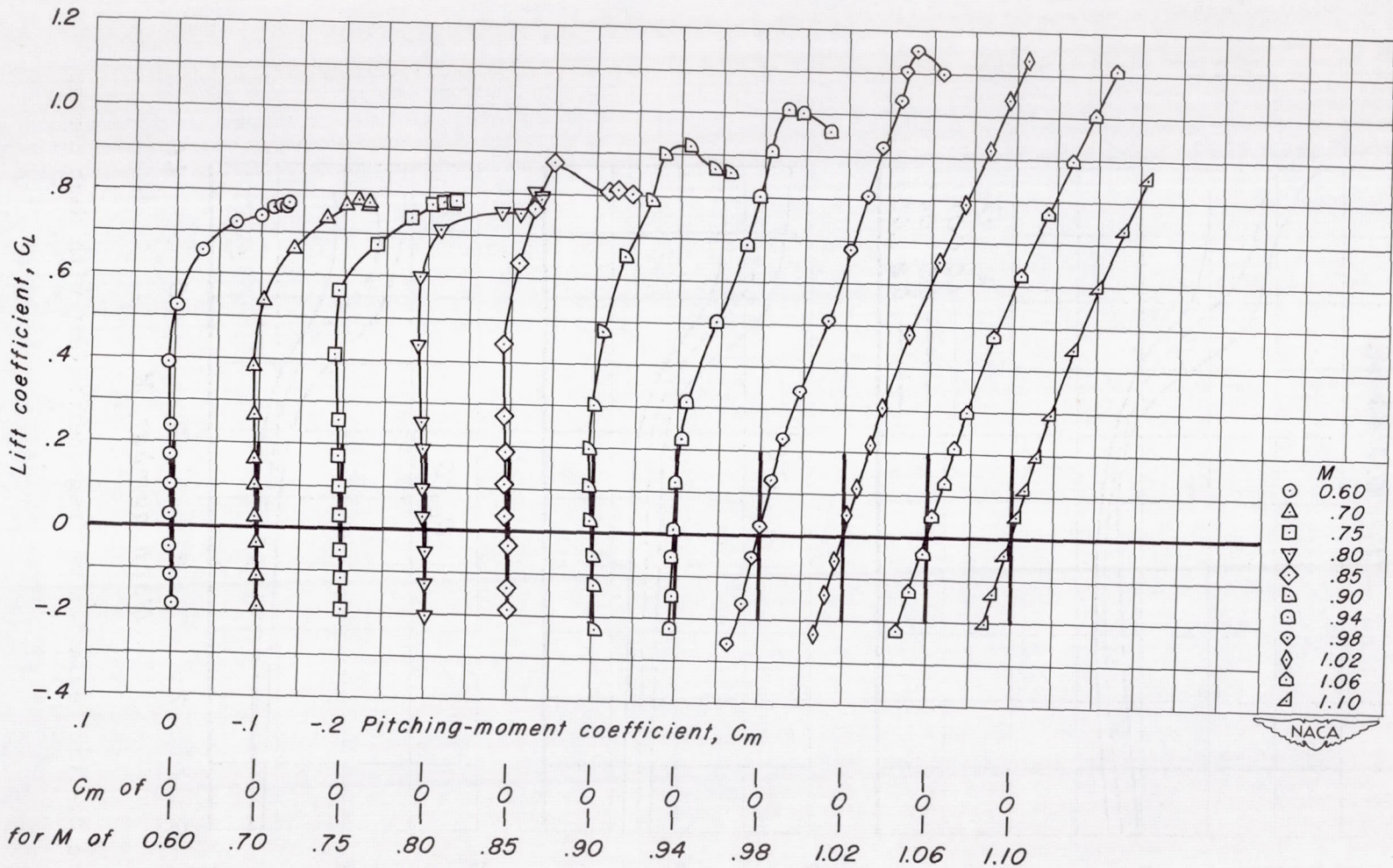
CONFIDENTIAL



(b) Taper ratio = 0.5

Figure 7.- Continued.

CONFIDENTIAL



(c) Taper ratio = 1.0

Figure 7.- Concluded.

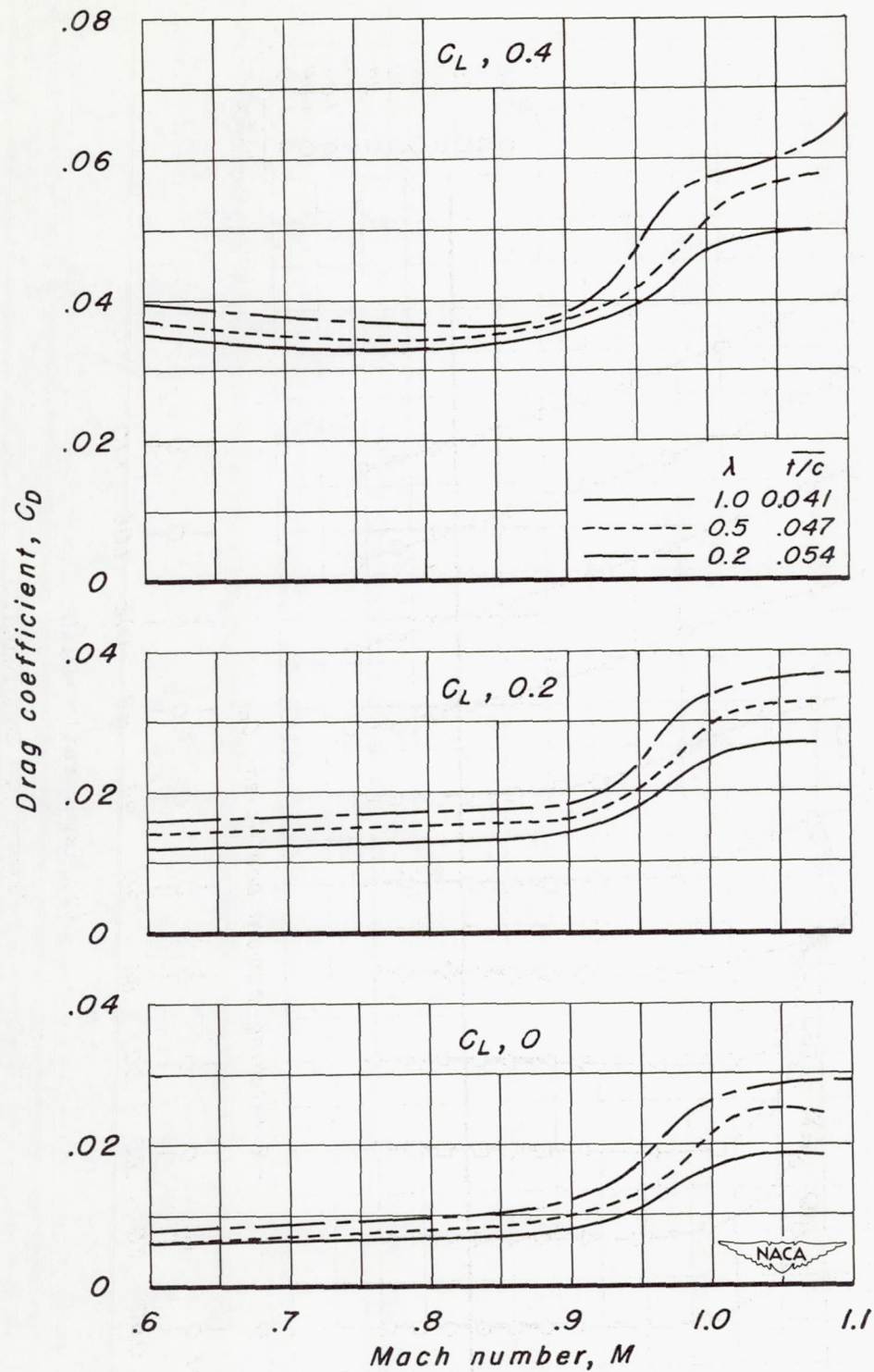


Figure 8.- The variation of drag coefficient with Mach number.

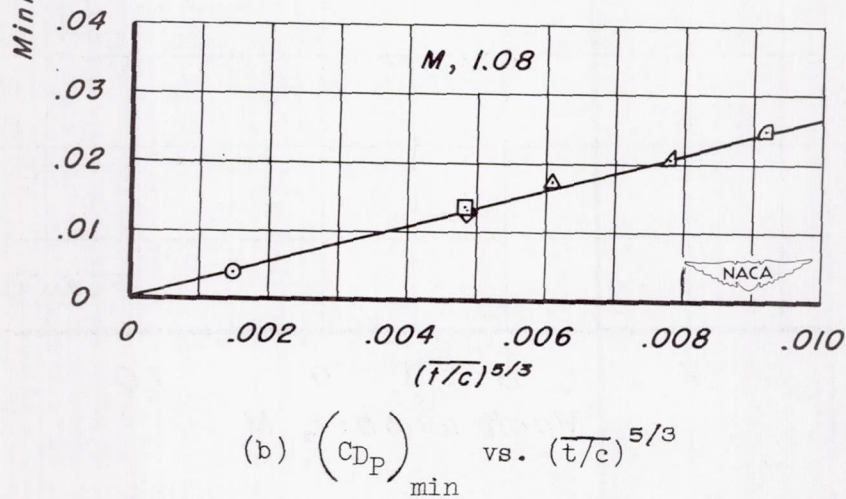
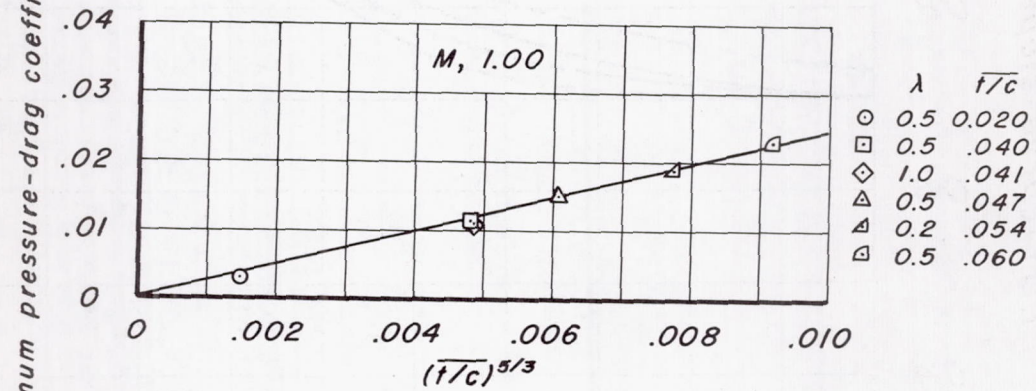
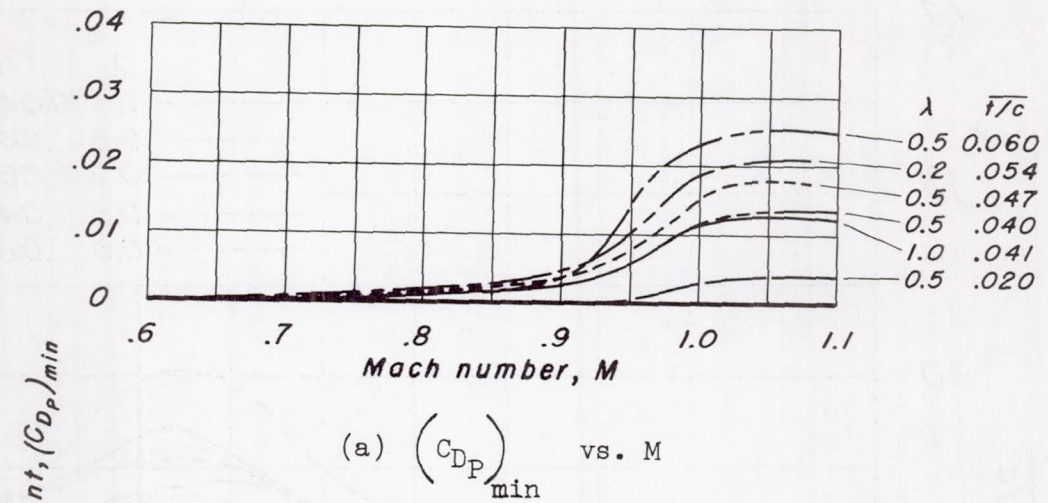


Figure 9.- The variation of pressure-drag coefficient with Mach number and thickness ratio.

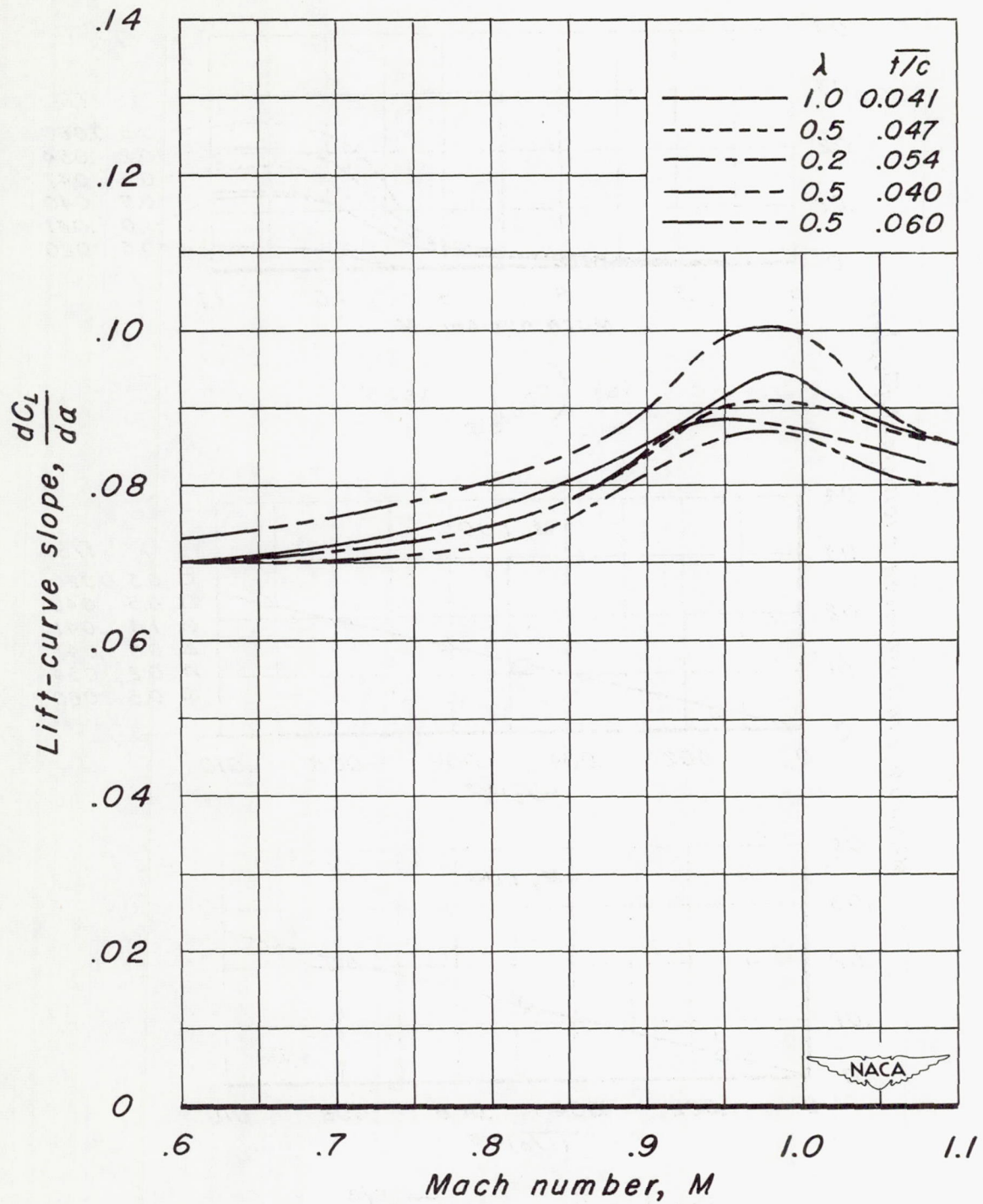
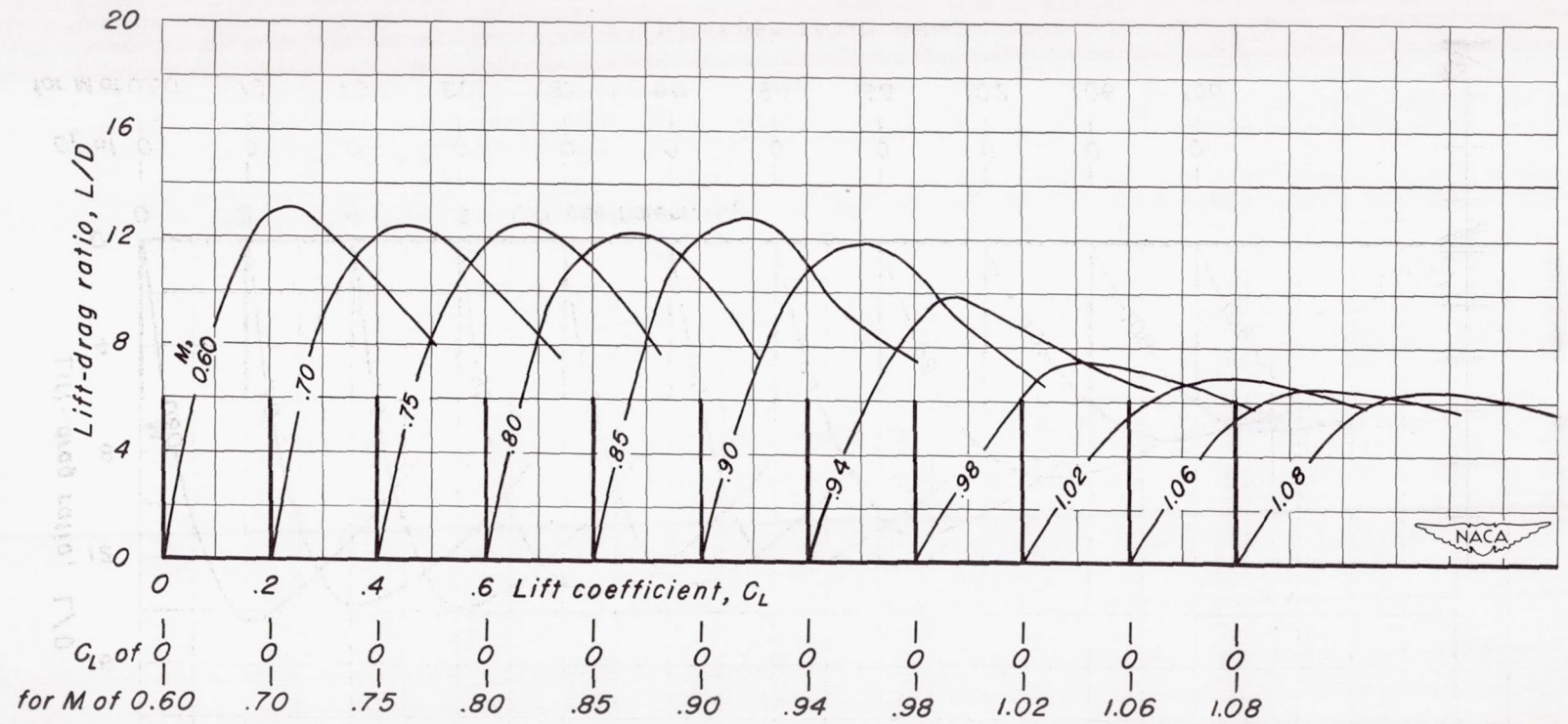


Figure 10.- The variation of lift-curve slope with Mach number.

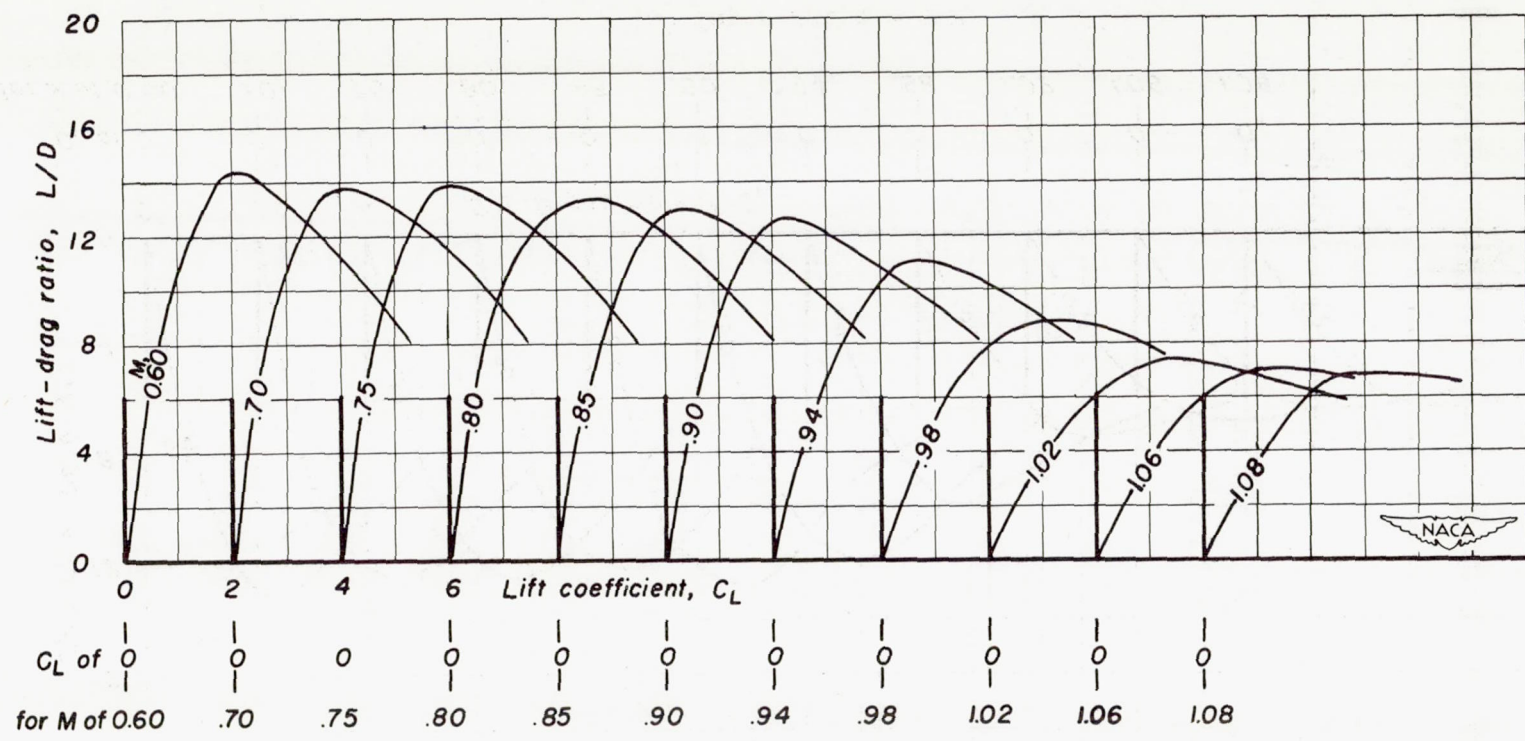
CONFIDENTIAL



(a) Taper ratio = 0.2

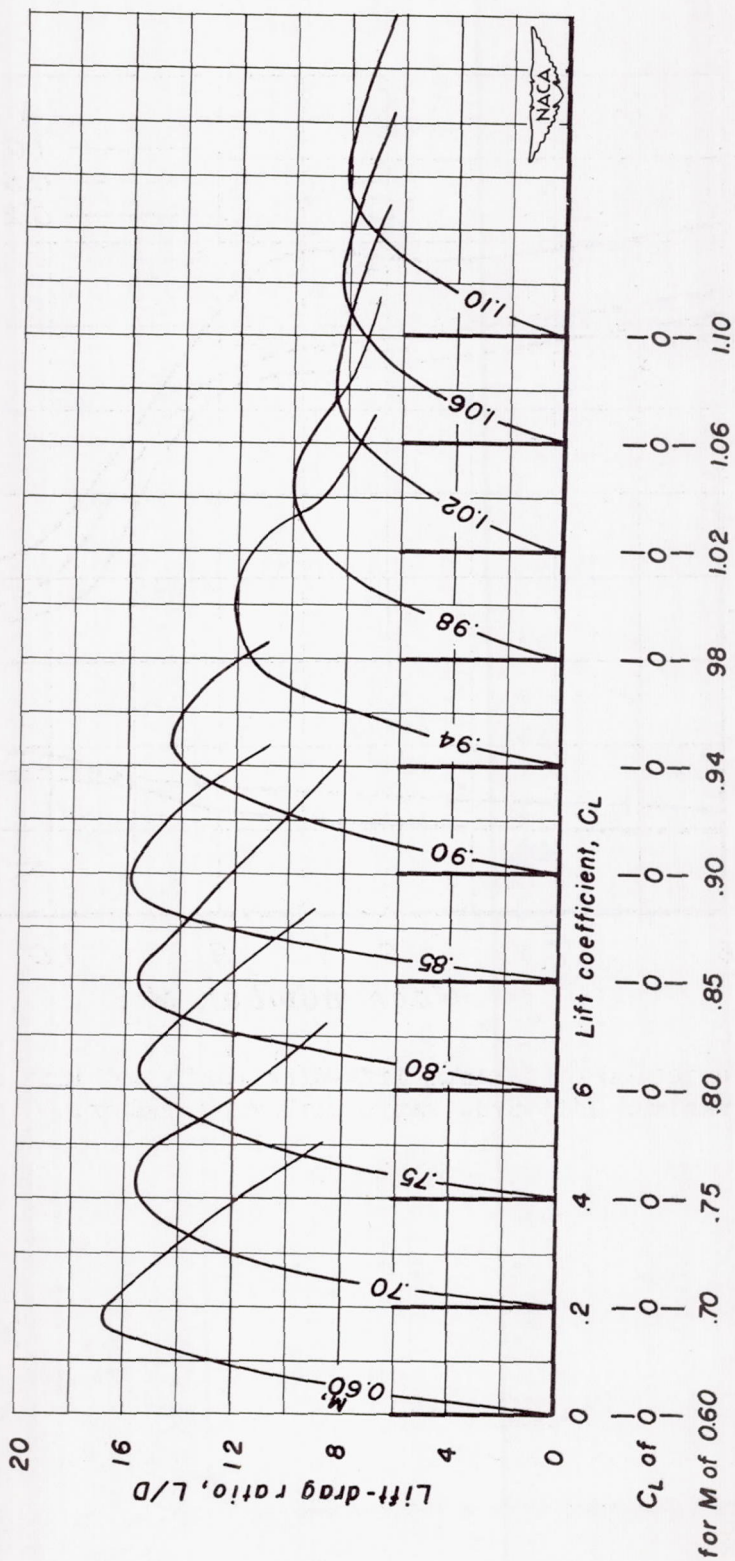
Figure 11.- The variation of lift-drag ratio with lift coefficient.

CL of 0 0 0 0 0 0 0 0 0 0 0
for M of 0.60 .70 .75 .80 .85 .90 .94 .98 1.02 1.06 1.08



(b) Taper ratio = 0.5

Figure 11.- Continued.



(c) Taper ratio = 1.0

Figure 11.- Concluded.

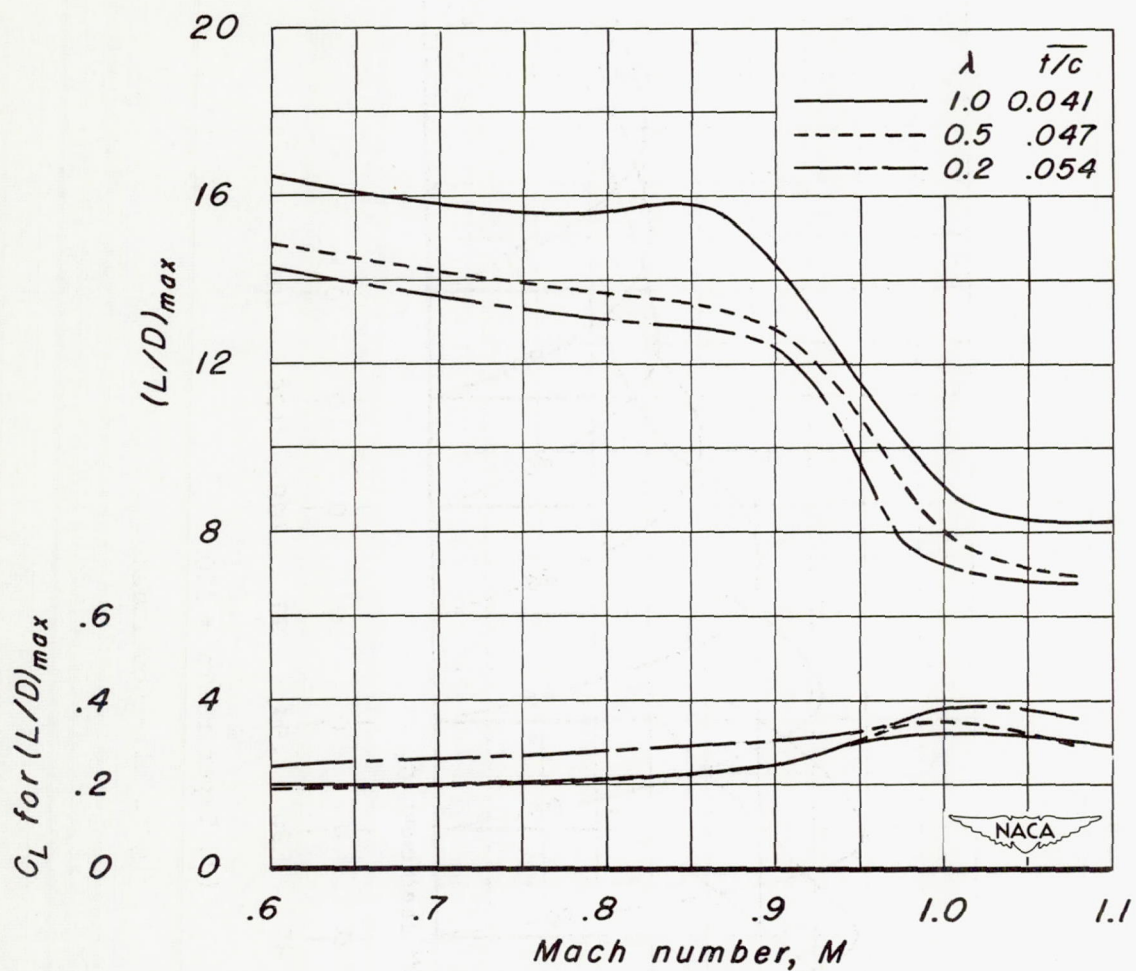


Figure 12.- The variation of maximum lift-drag ratio and lift coefficient for maximum lift-drag ratio with Mach number.

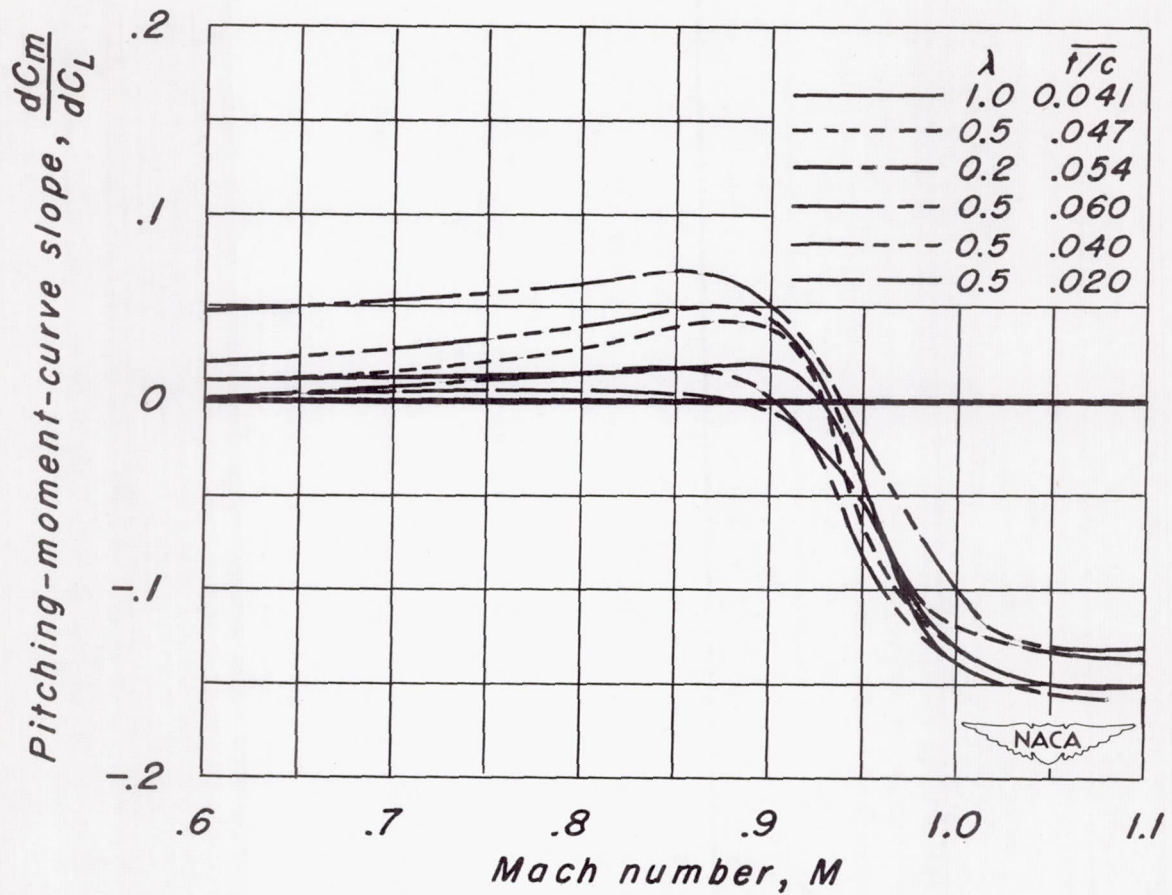
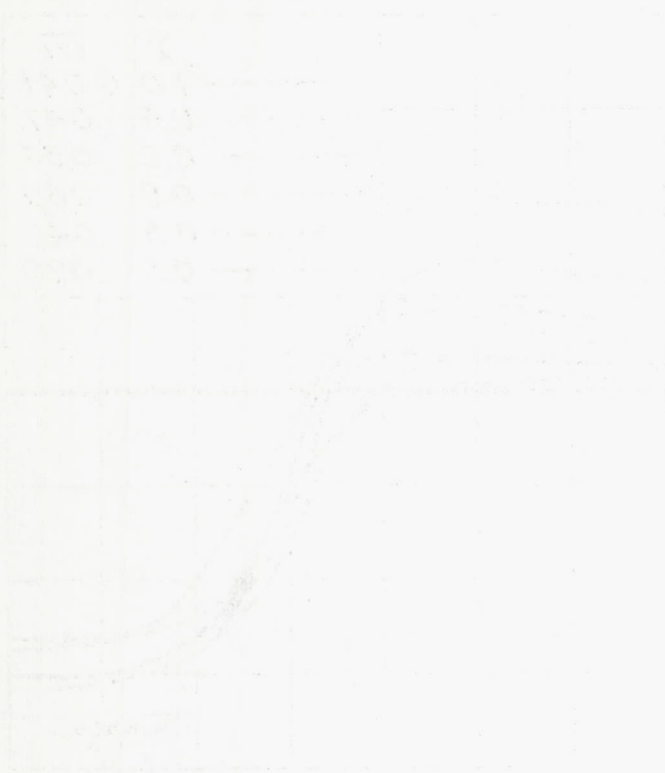
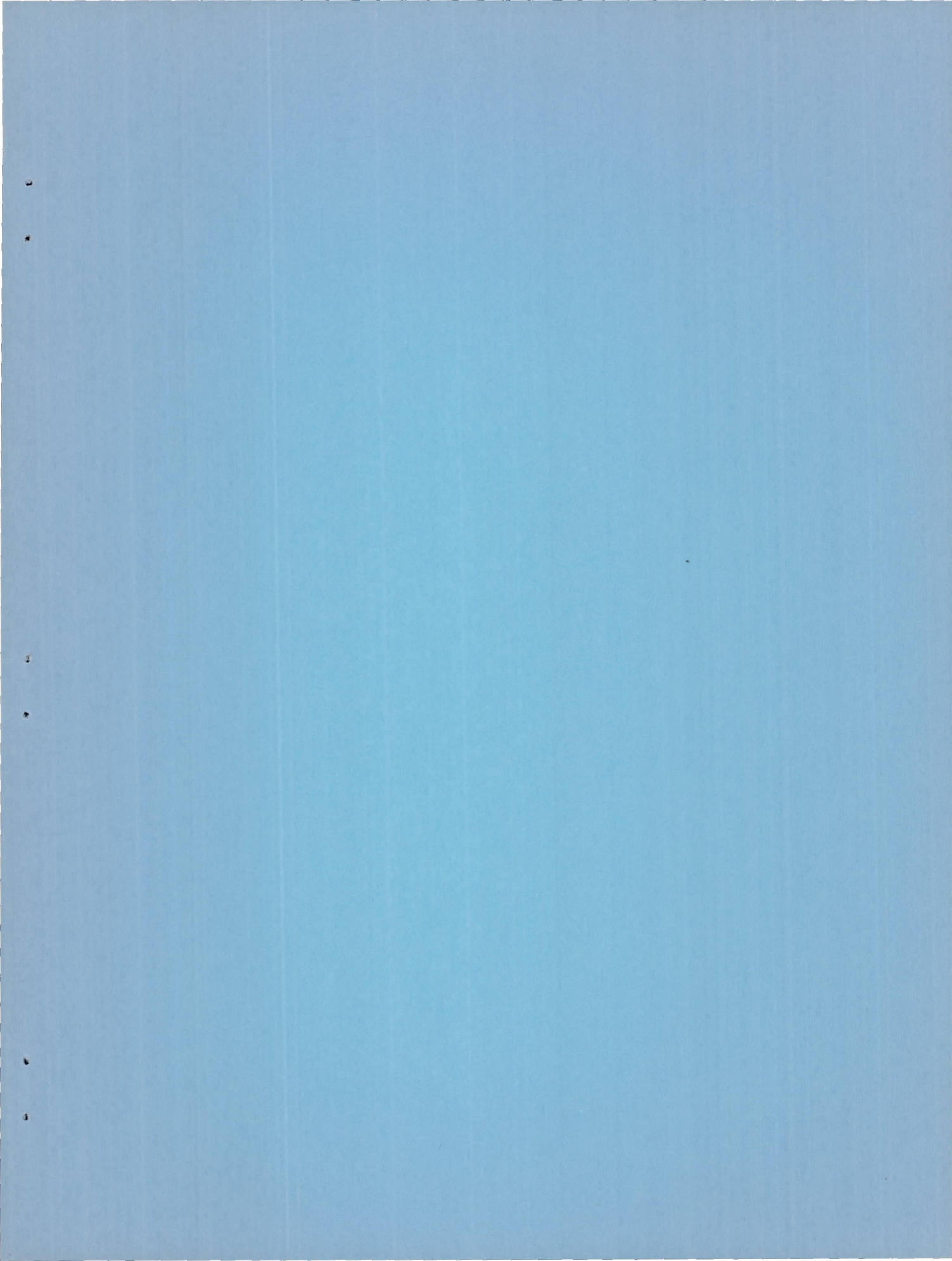


Figure 13.- The variation of pitching-moment-curve slope with Mach number.



Number

Time



CONFIDENTIAL

CONFIDENTIAL